DESIGN OF A MODULAR SPHERICAL ROBOT FOR SURGICAL APPLICATIONS

GABRIELA RUS[1], NADIM Al HAJJAR[2], CALIN VAIDA[1], FLORIN ZAHARIE[2], ALIN BURZ[1], NAGY JEFTE[1], ALEXANDRU PUSCA[1*], ANDREI CAILEAN[1*], NICOLETA POP[1], DOINA PISLA[1,3]

Abstract. The paper presents the design and experimental model of a spherical robot with dynamic balancing of the end-effector for highly accurate tasks covering medical applications. The robot is specially designed to perform different tasks based on the concept of the Remote Centre of Motion (RCM), suitable for the manipulation of objects located in a sealed environment with a specific access port. The specific advantages of an architecturally constrained RCM are demonstrated in terms of safety in operation, ease of control, and motion decomposition. The mechanism is balanced to allow a large working envelope with minimum torque variations for the actuators, improving both accuracy and stiffness. A case study is presented where the end-effector is represented by a dexterous surgical instrument, which adds four additional degrees of freedom to the gripper along demonstrating through a mathematical model the specific gains in accuracy and stiffness. Through computer-based simulations, the specific advantages of the balancing mechanism are illustrated along with a simple solution that enables the robot to adapt to different end-effectors and working loads. In addition to these aspects, the experimental model of the robot with command and control logic developed based on a master-slave architecture is also presented, which allows the surgeon to remotely control the instrument attached to the proposed solution.

Key words: Spherical robot, design and dimensional optimization, singularity-free workspace, experimental model, dynamic balancing.

1. INTRODUCTION

One major challenge in the development process of robots is related to stiffness, considering that this characteristic can affect the ability of the robot to interact with the environment. Robotic systems with high stiffness enable precise

[1] CESTER, Technical University of Cluj-Napoca, 400114 Cluj-Napoca, Romania
[2] Department of Surgery, "Iuliu Hatieganu" University of Medicine and Pharmacy, 400347 Cluj-Napoca, Romania
[3] Technical Sciences Academy of Romania, B-dul Dacia, 26, 030167 Bucharest, Romania

Ro. J. Techn. Sci. − Appl. Mechanics, Vol. 70, N° 1–3, P. 63–80, Bucharest, 2025

DOI:10.59277/RJTS-AM.2025.1-3.04

motion control, which is critical in high-precision applications such as Single-Incision Laparoscopic Surgery (SILS) and other minimally invasive procedures [1].

Based on a single incision through which the trocar is introduced, SILS provides many advantages, among which can be mentioned: shorter post-operative recovery, less hospitalization time, and better aesthetic outcomes. The introduction of robots in SILS [2] improved the medical act, enhancing the dexterity and precision of the surgeon, offering ergonomic improvements, expanding in this way the surgical capabilities [3]. Since the introduction of the da Vinci robotic system in 2000 [4], this area has been evolving at an accelerating rate, providing different architectural design configurations for robotic-assisted SILS. These design aspects and the definition of efficient and safe architectures have been analyzed in [5–7], papers that illustrate different design approaches used in defining a medically relevant structure. In addition to the challenges and methods of developing the design of these structures, another major issue is their dynamic behavior. Studies [8–9] present a series of dynamic balancing modes used in surgical robots.

Some of the well-known systems used for SILS procedures include the da Vinci SP robot (FDA approval in 2018 [10]), which features three fully wristed and elbowed instruments measuring 6 mm in size, along with an articulated 3D endoscopic camera measuring 8 mm in size. Another system used in SILS procedures is the Senhance system, which consists of four independent and exchangeable arms that can control three active instruments and a laparoscopic camera [11]. The CMR Versius system consists of three to four independent arms and a master console [12]. Within CESTER, the authors have also investigated the development of modular parallel architectures that manipulate a mobile platform, which holds all the surgical instruments [13–14].

Current solutions often involve complex mechanical structures, limited modularity, or high actuation forces, which can affect precision, safety, or adaptability during different procedures such as pancreatic or esophageal surgery.

To address these limitations, this paper proposes a novel modular spherical robotic system designed specifically for SILS procedures on the pancreas and esophagus. The robot features a kinematically constrained RCM to ensure precise and safe instrument manipulation. By integrating a dynamic balancing mechanism, the system significantly reduces actuator torque while improving stiffness and stability, making it suitable for high-accuracy surgical operations in confined anatomical spaces.

The paper is structured as follows: Section 1 introduces the clinical context and outlines the main challenges of robotic-assisted Single-Incision Laparoscopic Surgery (SILS). Section 2 presents the design requirements and the kinematic scheme of the proposed modular spherical robot, including its RCM-based motion constraint. Section 3 details the CAD model and design parameters, while Section 4 focuses on the dynamic analysis and the implementation of the balancing mechanism. Finally, Section 5 discusses the main conclusions and outlines directions for future work.

2. DESIGN CHARACTERISTICS OF THE MODULAR ROBOT

To achieve the specific requirements of a surgical structure [15–16], which include precision, dexterity, safety, and compatibility with medical procedures, it is essential to identify the appropriate design that fulfils these criteria. Understanding the constraints associated with these requirements becomes vital in this process.

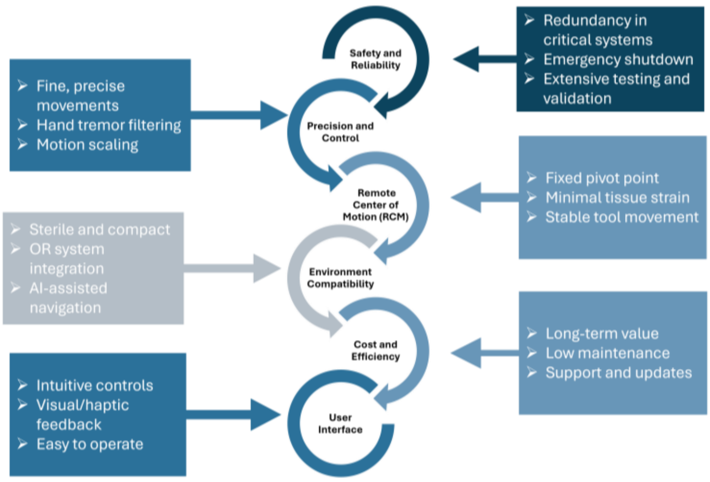

Fig. 1 – Key features of a surgical robotic system.

Fig. 1 illustrates key design features of a surgical robotic system that address essential clinical requirements such as precision, dexterity, safety, and system integration. Each element contributes to enhancing performance in the operating room while ensuring reliability and ease of use.

A particular characteristic of any robotic structure developed for a minimally invasive surgical procedure is its motion with respect to the entry point inside the body [17]. This point is known as RCM and was introduced for the first time in 1997 by Russel Taylor. Kinematically, this point is defined as a fixed point in the robot workspace, which is located along the longitudinal axis of the instruments inserted inside the body. The RCM can be obtained in three ways:

1. Using a **2-degrees of freedom (DOF) passive joint** in the attachment point of the instrument to the robotic arm – this is the simplest approach, but it is limited to the manipulation of instruments which have no contact with the internal organs, as they are guided by the constraint (passive joint) of the tissue surrounding the entry port;

2. Using an additional **2-DOF active joint** for the manipulation of the instruments – these two additional active movements are used to compensate any displacements of the instrument relative to the entry point; this approach increases the complexity of the mechanical structure and the control algorithms, and in case of failure there is a high risk of injury for the patient;

3. Using a robot architecture that **constraints kinematically the entry point** inside the body using different mechanisms – this approach imposes a very good alignment between the robot and the patient before the instruments insertion but ensures a safe behavior throughout the surgery.

To determine the critical design parameters of the robotic structure, an Analytic Hierarchy Process (AHP) analysis was performed based on a set of characteristics required for SILS (1–7), and the results are presented in Fig. 2.

(1) – **Modularity**: the design must accommodate the use of either one or multiple spherical arms in different configurations, even with other robotic devices [18].

(2) – **Stiffness**: the design must ensure good stiffness in the entire operational workspace, avoiding spikes in torques or reaction forces.

(3) – **Dexterity**: maximized operational workspace with similar positional increments throughout it.

(4) – **Actuation forces**: minimal actuation forces, equally distributed in the operational workspace.

(5) – **Operating room (OR) integration**: the robot should have a small footprint to accommodate the different OR configurations.

(6) – **Minimum occupied volume**: the robot should occupy a minimal volume concerning the sides of the spherical arm, to enable efficient multi-arm integration.

(7) – **Instruments compatibility**: the robot must be able to manipulate several types of instruments, from active ones to different 2D and 3D endoscopic cameras.

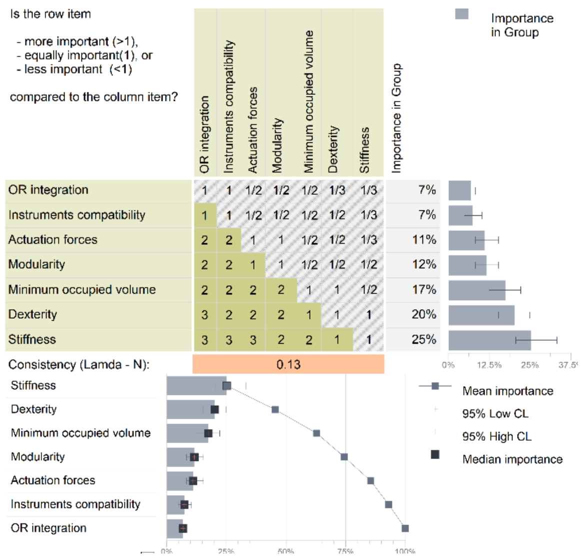

Fig. 2 – AHP analysis of the design requirements.

2. 1. KINEMATIC SCHEME

Based on characteristics defined in the previous section, the proposed robotic system is designed according to the third RCM configuration, namely by kinematically constraining the entry point inside the body.

Thus, the SILS robotic system consists of a 3-DOF translational module and three independent spherical modules with various geometric parameters defining their relationships and movements. The relative positioning of the three spherical arms is consistent with the specialized SILS ports, where a small distance (of 5 to 10 mm) is required between the RCM_s of each arm, while the spatial translational modules ensure the positioning of the entry ports concerning the patient.

The kinematic scheme of the complete spherical robotic system is presented in Fig. 3.

In the multi-arm configuration, the SILS robotic system consists of a single translational module on which three spherical modules are positioned: the lateral ones (left *l*, right *r*) are used for the manipulation of the active instruments, and the central one is used to position the endoscopic camera (*e*). For kinematic modelling, a fixed coordinate system (*OXYZ*) is defined at the base of the translational modules, and three mobile coordinate systems ($O_lX_lY_lZ_l$ – left spherical module, $O_eX_eY_eZ_e$ – endoscopic camera, and $O_rX_rY_rZ_r$ – right spherical module) are each attached at the tip of each surgical instrument.

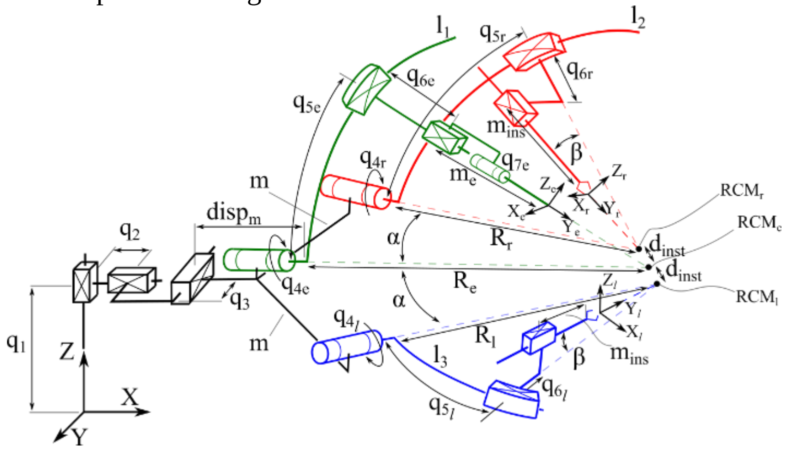

Fig. 3 – The kinematic scheme of the SILS modular robotic structure.

The modular robotic system consists of:

– **The Cartesian module** – a 3-DOF Cartesian mechanism with the role of guiding the mechanical element *m* (the mounting base for the three spherical modules), which has three active joints: q_1, q_2, q_3.

– **The Spherical modules for active instruments** are mounted on a mechanical element *m*, on either side of the endoscope. Both modules feature 3-

DOF, which are controlled by revolute joints (q_{4r}, q_{4l}), and translational joints (q_{5r}, q_{5l} – along the curved links, respectively q_{6r}, q_{6l}).

– **The Spherical module for the endoscopic camera** is also mounted on a mechanical element *m* is a 4-DOF mechanism actuated by two revolute joints (q_{4e}; q_{7e}) and two translational joints (q_{5e}, q_{6e}).

The geometric parameters are defined for each module, including the rays (R_l, R_r, R_e), displacement ($disp_m$), distance between the RCM_s of the active instruments (*dinst*), the angle of rotation around *OZ* between the side arms and central one, denoted α, offset for instrument mounting β, and minimum insertion lengths (min_s, m_e) for the instruments and endoscopic camera, the *RCM* points for the active instruments and endoscope, denoted as RCM_l, RCM_r, and RCM_e, respectively. The circular mechanical links (l_1, l_2, l_3) are actuated on arcs with centres at RCM_l, RCM_r, and RCM_e, respectively.

For the subsequent analysis, a consistent notation of joint coordinates and structural parameters is adopted.

Symbol	Definition
q_1, q_2, q_3	Cartesian module active joints
q_{4l}, q_{4r}, q_{4e}	Revolute joints of the spherical modules (left, right, endoscopic camera)
q_{5l}, q_{5r}, q_{5e}	Translational joints along the spherical module arcs
q_{6l}, q_{6r}, q_{6e}	Additional translational joints for tools and the camera
q_{7e}	Additional revolute joint for the endoscopic camera
d_{ispm}	Displacement of the mechanical base platform
d_{inst}	Distance between the RCM points of the instruments
m_{ins}, m_e	Minimum insertion lengths (for instruments and endoscopic camera)
R_l, R_r, R_e	Radii of the spherical modules (left, right, endoscopic camera)
RCM_l, RCM_r, RCM_e	Remote Center of Motion points (left, right, endoscopic camera)
l_1, l_2, l_3	Mechanical circular links of the spherical structure
α	Rotation angle around the OZ axis between the lateral and central arms
β	Mounting offset for the instruments

The detailed geometrical model of the robotic system is presented in [19], the final, fully parametric expressions being illustrated below:

The Cartesian positioning module:

$$\begin{cases} q_1 = Z_{RCM}, \\ q_2 = Y_{RCM} - R_e - disp_m, \\ q_3 = X_{RCM}. \end{cases} \tag{1}$$

The spherical modules:

$$\begin{cases} q_{4\_l} = \theta_l + \beta, \\ q_{5\_l} = R_l \cdot \left(\psi_l + \dfrac{\pi}{2} \right), \\ q_{6\_l} = \left(R_l - m_{ins} \right) + ins_l, \end{cases} \quad \begin{cases} q_{4\_e} = \theta_e, \\ q_{5\_e} = R_e \cdot \left(\psi_e + \dfrac{\pi}{2} \right), \\ q_{6\_e} = \left(R_e - m_e \right) + ins_e, \\ q_{7\_e} = \varphi_e. \end{cases}$$

$$\begin{cases} q_{4\_r} = \theta_r - \beta, \\ q_{5\_r} = R_r \cdot \left(\psi_r + \dfrac{\pi}{2} \right), \\ q_{6\_r} = \left(R_r - m_{ins} \right) + ins_r, \end{cases} \tag{2}$$

where

$$\theta_l = \operatorname{sgn}\left(Z_{RCM\_l} - Z_{l\_rot} \right) \cdot \operatorname{sgn}\left(-X_{l\_rot} \right) \cdot$$
$$\cdot \operatorname{atan2}\left(\left| X_{l\_rot} \right|, \left| Z_{RCM\_l} - Z_{l\_rot} \right| \right),$$
$$\psi_l = \operatorname{sgn}\left(Z_{RCM\_l} - Z_{l\_rot} \right) \cdot \operatorname{sgn}\left(Y_{RCM\_l} - Y_{l\_rot} \right) \cdot$$
$$\cdot \operatorname{atan2}\left(\left| Y_{RCM\_l} - Y_{l\_rot} \right|, \frac{\left| Z_{RCM} - Z_{l\_rot} \right|}{\cos\left(\theta_l \right)} \right),$$
$$ins_l = \operatorname{sgn}\left(Z_{RCM\_l} - Z_{l\_rot} \right) \cdot$$
$$\cdot \sqrt{X_{l\_rot}^{\,2} + \left(Y_{RCM\_l} - Y_{l\_rot} \right)^2 + \left(Z_{RCM\_l} - Z_{l\_rot} \right)^2}.$$

Figure 4 illustrates the main stages of the surgical procedure and the corresponding robot modules involved at each step. The process begins with the robot–patient registration, which is carried out using only the Cartesian module (joints q_1, q_2, q_3). This ensures that the RCM points are precisely positioned and remain fixed throughout the entire procedure, ensuring a safe setup. During the instrument insertion phase, the spherical modules (joints q_4 to q_7) are activated to align and position the instruments along the constrained paths defined by the RCM_s. Finally, in the surgery phase, the active instruments, mounted on the spherical modules and offering 4 additional degrees of freedom, are controlled to perform the required surgical tasks. By decoupling the actuation between the Cartesian module and spherical modules and limiting the movement of active instruments within the safe workspace, the system significantly enhances procedural safety and minimizes the risk of patient injury even in the event of operator error.

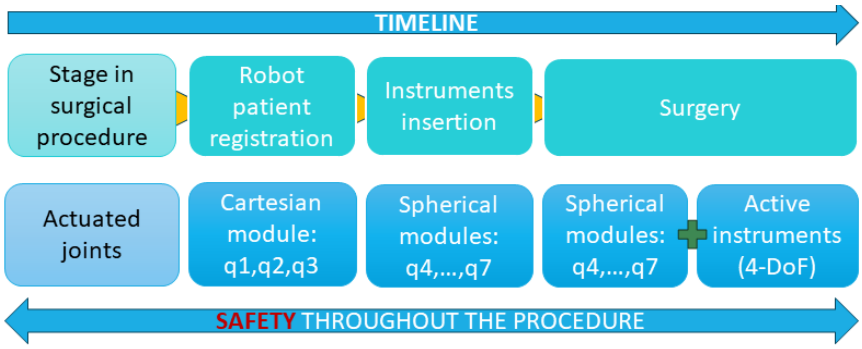

Fig. 4 – Main surgery steps.

3. DESIGN OF THE SPHERICAL ROBOT

3. 1. CAD MODEL

Based on the AHP analysis, the final design of the spherical robot was defined with respect to the kinematic scheme.

Starting from the positioning of the modular arms (on which the endoscopic camera and the active instruments are mounted), it has been determined that implementing dimensional constraints can aid in determining the optimal size of the surgical robot. To achieve this, adopting a vertical axis design is deemed suitable, as it offers the advantage of occupying minimal workspace in the operating room. The size of the spherical arm is defined based on the existing instrumentation (active instruments with a total length of 450–570 mm, endoscopic camera 210–450 mm), imposing the use of a spherical rail with a radius of 600 mm.

The instrument case is attached to the linear carriage using a linear profile oriented such that the instrument's longitudinal axis will always pass through the centre of the rail. This alignment is essential for accurate and precise movements during the surgical procedure. Additionally, the use of spherical modules helps maintain a consistent gripping force within the robot's operational workspace.

By combining these design considerations and constraints, the surgical robot can optimize its size and functionality while adhering to key architectural requirements. This approach ensures efficient use of space in the operating room and enables precise and safe surgical interventions.

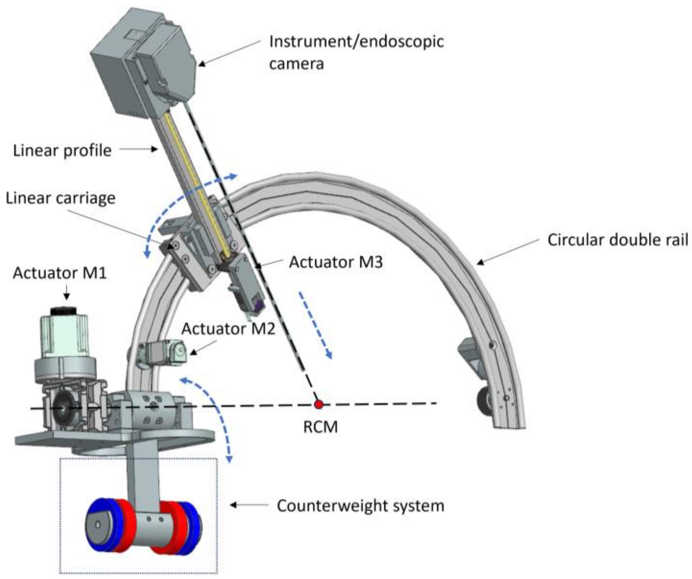

Fig. 5 – The 3D model for the SILS spherical robot.

Figure 5 presents the CAD model of a single spherical robotic module, designed to manipulate a surgical instrument or endoscopic camera concerning a fixed RCM. The structure consists of the following components:

– Actuator *M1* enables rotational motion around a fixed horizontal axis, defining one rotational movement about the center of the spherical rail.
– Actuator M2 drives the linear carriage along the circular double rail, providing a second rotational movement concerning the same spherical surface.
– Actuator M3 enables a linear translation along the instrument's longitudinal axis, through a linear profile, allowing insertion or retraction of the instrument relative to the RCM point.
– The circular double rail constrains the motion of the linear carriage to a predefined arc, ensuring motion along a spherical surface centered at the RCM.
– The linear carriage supports the instrument and transmits the motion induced by actuators M2 and M3.

The linear profile ensures the alignment of the instrument axis with the RCM throughout motion.

The RCM is defined as the intersection point through which the instrument's axis must pass during all motions, ensuring minimally invasive access through a fixed entry port.

The counterweight system provides dynamic balancing relative to actuator *M1*, compensating for gravitational effects and minimizing torque requirements during motion.

The combined actuation of *M1* and *M2* constrains the instrument to a spherical trajectory centered at the RCM, while *M3* ensures controlled axial translation.

3. 2. DYNAMIC ANALYSIS

Considering the nature of the surgical operation performed by the spherical robot, a dynamic analysis was performed.

To study the dynamic behavior of the spherical module, a motion simulation was performed in Siemens NX software to determine the torque variation for the actuator *M1*. A harmonic motion was applied as the input to the active revolute joint, with an amplitude of 60° (which is the maximum inclination of the active instruments in SILS) and a frequency of 100 °/s. The resulting torques generated by the joint were recorded and illustrated in Fig. 6. This approach allows for a comprehensive analysis of the torque profiles and behavior exhibited by the spherical module in response to the applied harmonic motion.

As can be seen in Fig. 6, the result obtained revealed that the driving torque required for the *M1* actuator has a peak of 7.7 Nm.

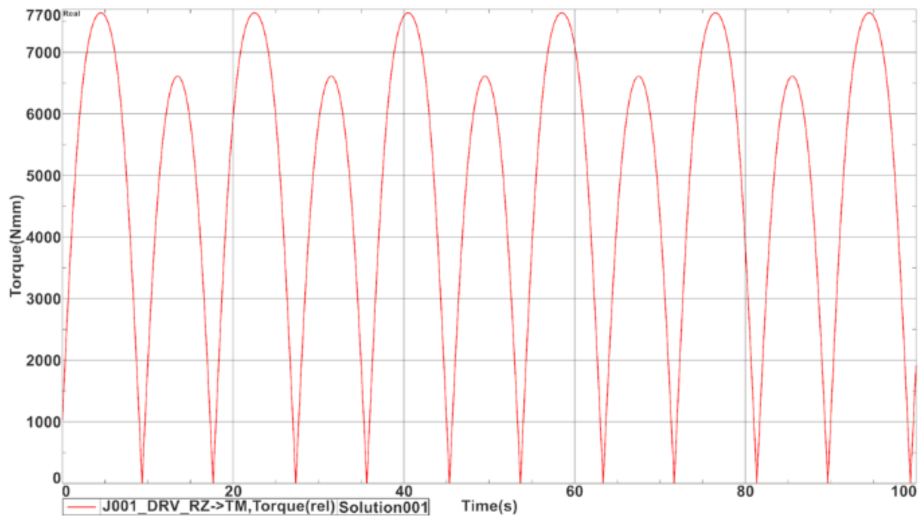

Fig. 6 – Torque values during revolute motion without the counterweight system.

To rectify this behavior, a counterweight mechanism was added to minimize this torque. The primary purpose of this mechanism is to effectively counterbalance the load of the instrument in a dynamic way (the effect of the balancing mechanism is proportional to the inclination angle). This can reduce wear and tear on the motor, enabling the use of a smaller actuator, also improving motor performance and conserving energy. Figure 7 illustrates the torque variation for the same simulation parameters. The maximum torque is now 3.5 Nm, which is over 2 times lower than in the initial situation.

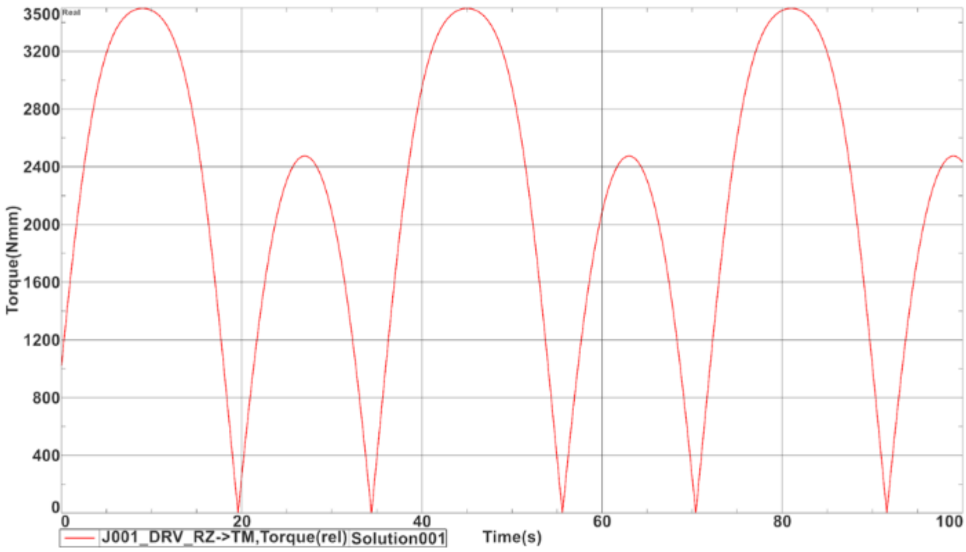

Fig. 7 –Torque values during revolute motion without the counterweight system.

4. EXPERIMENTAL MODEL OF THE SILS SPHERICAL ROBOT

The experimental model of the spherical robot developed for SILS surgery was based on the 3D model presented above. To ensure robust control and safety in the use of the structure, industrial equipment was used in the command and control logic, developed by B&R Industrial Automation. The control and command logic developed is based on the master-slave concept [16], whereby the surgeon manipulates the robot via a master console consisting of a 3D Space Mouse peripheral device that provides 6-DOF, to which is added the option to control the robot via a keyboard and mouse. The master-slave concept used to control the SILS spherical robot is illustrated in Fig. 8.

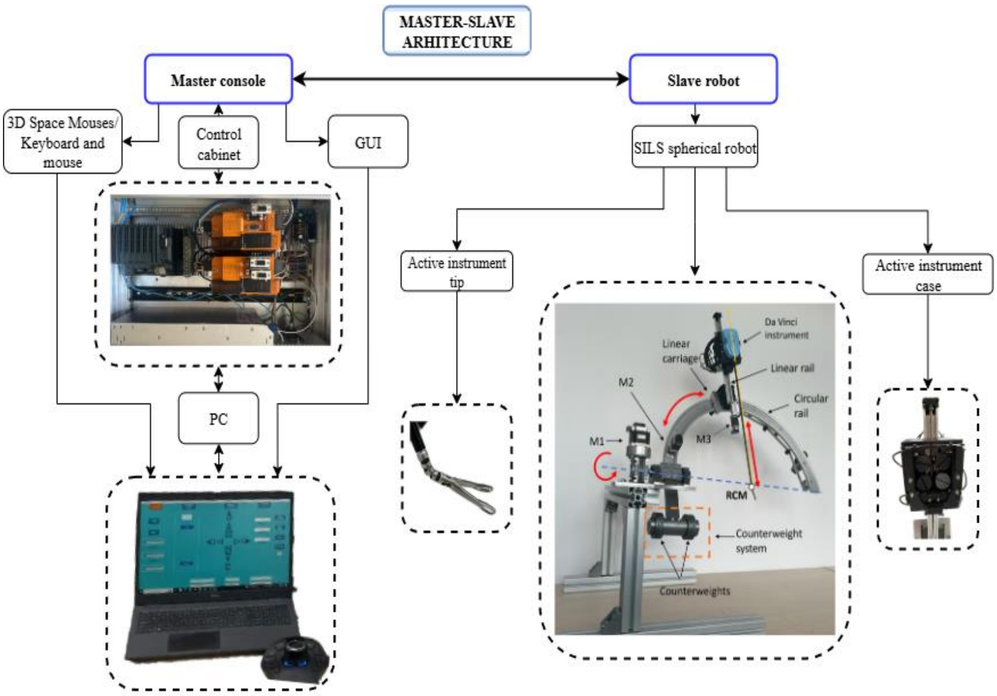

Fig. 8 – Master-slave concept of the SILS spherical robot.

Based on the master-slave architecture presented in Fig. 7, the command and control architecture of the SILS spherical robot was implemented on three main levels, namely: user level, command and control level, and physical level. A detailed view of the three levels is presented in Fig. 8, with input data transferred from the user level (the surgeon's hand) to the command and control level via a 3D Space Mouse (6-DOF), where the data is process, convert, and transfer to the physical level of the SILS spherical robot, thus reproduces the surgeon's hand movement in real time and on a 1:1 scale. This is possible due to the robust industrial equipment used for command and control, with the programmable controller used (B&R X20CP1684 PLC) having an information processing time of less than 5 milliseconds.

The experimental model of the SILS spherical robot is controlled in two phases. The first phase involves controlling the three actuators mounted on the spherical arm structure, which perform one rotational motion (enabling the orientation of the arm that supports the active instrument) and two translational motions (one performed along the circular rail using a belt drive, while the second translational motion is performed using a ball screw slide).

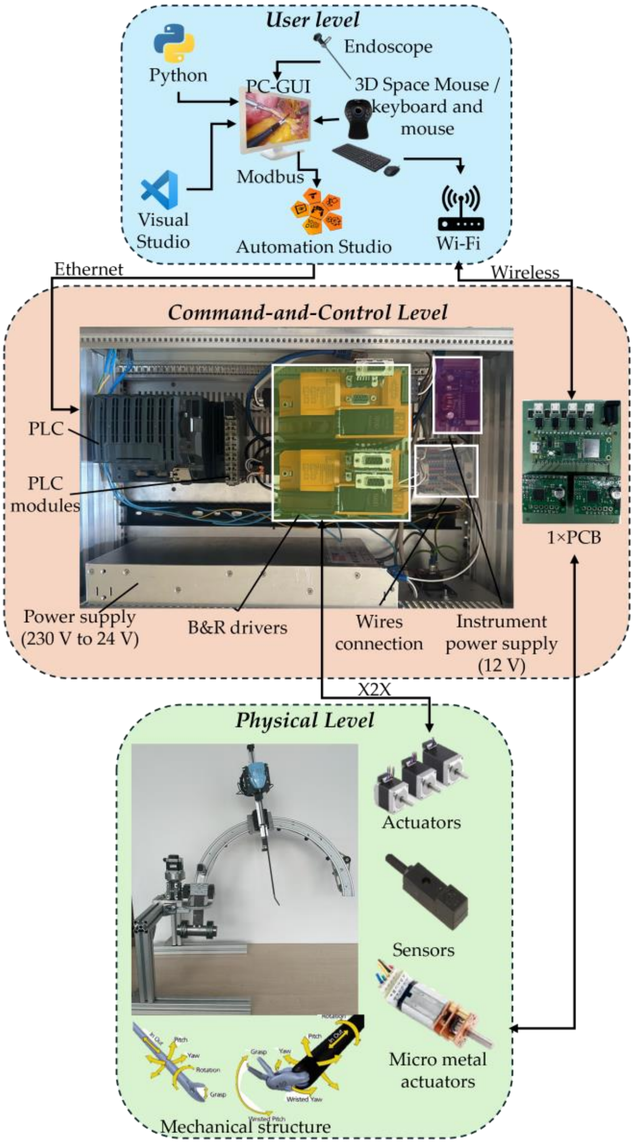

Fig. 9 – Hardware configuration of the SILS spherical robot.

Phase two of control is focused on controlling the active instrument mounted on the SILS spherical robot. The switch between the two control modes is achieved using a button on the 3D Space Mouse, which can be configured according to the surgeon's needs, so that after the desired orientation and insertion, the surgeon can push the button to switch to instrument tip control. To control the tip of the active instrument, four motors are used, covering the entire range of movements required by the surgeon. A detailed illustration of the movements that can be performed by the proposed solution is shown in Fig. 10.

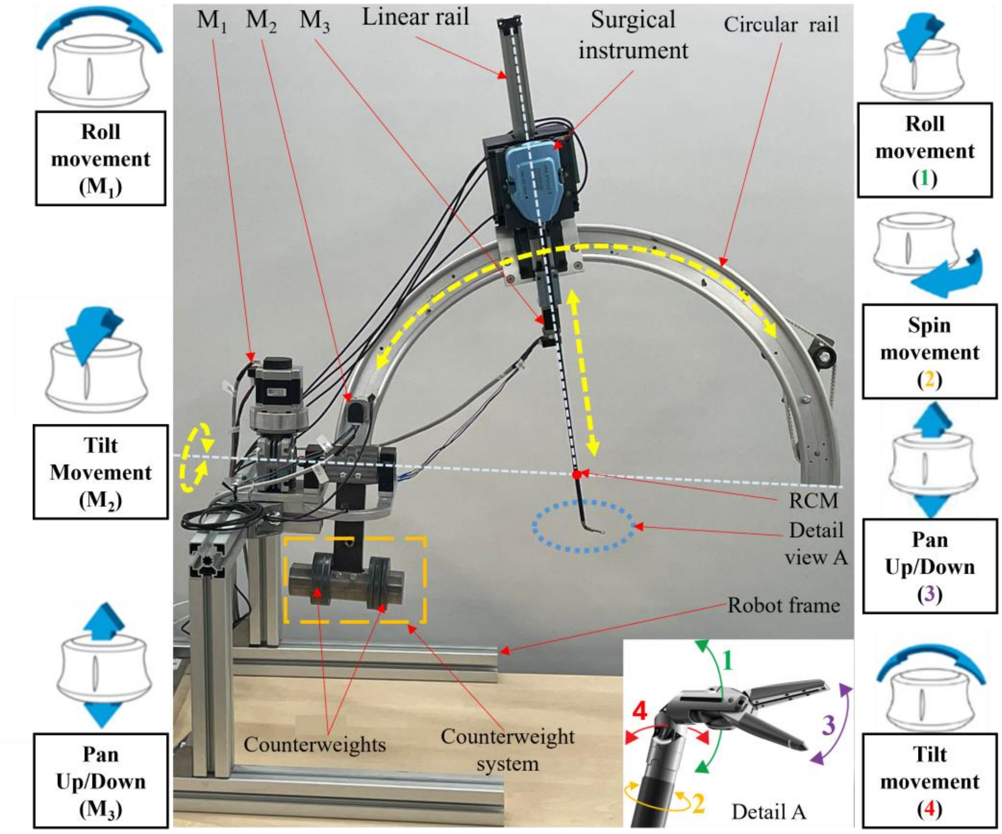

Fig. 10 – Range of motion of the SILS spherical robot.

The movements that the tip of the active instrument can perform after switching to the second control mode are: adduction/abduction (1), Z-axis rotation (2), grasping (3), and flexion/extension (4). These movements are correlated with the movements of the 3D Space Mouse and are illustrated in Fig. 10.

In order to contextualize these limitations, Table 1 summarizes the information that is publicly available for da Vinci SP, Versius, and Senhance systems. While the literature often points to issues such as mechanical complexity, limited modularity, or high actuation forces, manufacturers do not disclose quantitative engineering metrics such as stiffness, actuator torque, or absolute accuracy. This lack of transparency has been highlighted in recent reviews and underscores the relevance of our contribution, which provides experimental data for these parameters in the proposed spherical robotic arm.

Table 1

Comparative overview of state-of-the-art robotic surgery systems

System	Instruments and Ports	Architecture & Modularity	Reported Features in Literature	Footprint / Dimensions
da Vinci SP (Intuitive Surgical)	Up to 3 articulated instruments + 3D endoscope through 25 mm cannula; ≥10 cm working distance [20–21]	Single-port system, one patient cart, multi-articulated intracavitary arm [20]	High intracavitary flexibility; widely adopted in urology/gynecology; no stiffness/torque data disclosed	Patient cart approx. 104 × 178 × 204 cm [21]
Versius (CMR Surgical)	5 mm wristed instruments, 10 mm 3D camera; independent BSUs [22]	Modular: each BSU on a separate cart; open console	Emphasis on modularity and portability; cost-efficiency; no quantitative engineering data published	BSU footprint 38 × 38 cm, height 1425 mm [23]
Senhance (Asensus Surgical)	3 mm and 5 mm instruments, optional 7-DOF articulation (tip deflection 63°); haptic + eye-tracking [24]	Modular arms on carts, open cockpit console	Incorporates haptics and eye-tracking; pediatric applications; no accuracy/stiffness values published	Equipment cart 85 × 73 × 176 cm
Proposed spherical robotic arm (this study)	Single-port access; modular setup; interchangeable end-effectors	Spherical configuration with 3 DOF; compact design; simplified mechanics	Designed to reduce mechanical complexity and actuation forces, enhancing adaptability	Prototype bench-top footprint: 39x35x70 (measured)

5. DISCUSSION AND CONCLUSIONS

The design of a robot that meets the rigorous requirements for surgery and also responds to the challenges in this field was developed and presented in this study. For the development of this robot integrated into SILS (Single Incision Laparoscopic Surgery) robotic-assisted surgery, crucial factors such as rigidity, safety, and space efficiency were considered. The robot design process includes an AHP (Analytic Hierarchy Process) analysis, which facilitated the examination of key characteristics essential for the design of a robot intended for the field of surgery, with its integration into pancreatic surgery.

In addition, a dynamic analysis was performed by simulating the SILS spherical robot, in which the torque variation was monitored without and with the compensation element attached to the robot structure, which contributed to investigating the dynamic behavior of the proposed spherical module. This analysis provided important information about the module's performance during operation, with the torque obtained with the compensation element attached to the robot being significantly reduced (reduced by 2 times). Subsequently, an optimization process was undertaken to improve the functionality and efficiency of the module.

Although a complete tolerance analysis is beyond the scope of this paper, a preliminary estimation based on joint resolution, structural assembly tolerances, and control tracking indicates that the accumulated positioning error at the instrument tip is expected to remain below 0.5 mm within the central workspace. This order of magnitude is consistent with accuracy values reported for state-of-the-art robotic surgical systems. Furthermore, previous validation of the control architecture for the same spherical module [25] has demonstrated close agreement between simulated and experimental joint trajectories, which further supports the capability of the system to achieve sub-millimetric accuracy in practice

In addition to these aspects, the paper also covers the development of a command and control architecture based on the master-slave principle, whereby the surgeon transmits data collected through hand movements in real time to the active instrument attached to the robot, thus enabling the surgeon to remotely operate the robot's mechanical structure.

Based on this master-slave concept, the hardware part of the robot was developed and presented in the paper. It is divided into three levels, illustrating how the robot works and the movements it can perform.

All these advances are aimed at meeting the demanding requirements of the field of surgery, as well as optimizing the robot's performance in critical tasks.

Future work will involve a detailed mathematical analysis of the balancing mechanism to determine the optimal additional weight for different configurations and manipulated instruments, as well as the integration of a haptic device able to provide feedback to the surgeon during manipulation of the active instrument attached to the SILS spherical robot.

Acknowledgements. This research was supported by the project “New smart and adaptive robotics solutions for personalized minimally invasive surgery in cancer treatment” – ATHENA, funded by European Union – NextGenerationEU and Romanian Government, under National Recovery and Resilience Plan for Romania, contract no 760072/23.05.2023, code CF 116/15.11.2022, through the Romanian Ministry of Research, Innovation and Digitalization, within Component 9, investment I8 and by the project “Romanian Hub for Artificial Intelligence – HRIA, Smart Growth, Digitization and Financial Instruments Program, MySMIS no. 334906.

Received on July 9, 2025

REFERENCES

1. TUCAN, P., VAIDA, C., HORVATH, D., CAPRARIU, A., BURZ, A., GHERMAN, B., IAKAB, S., PISLA, D., *Design and experimental setup of a robotic medical instrument for*

brachytherapy in non-resectable liver tumors, Cancers, **14**, *23*, p. 5841, 2022, https://doi.org/10.3390/cancers14235841.

2. PANESAR, S., CAGLE, Y., CHANDER, D., MOREY, J., FERNANDEZ-MIRANDA, J., KLIOT, M., *Artificial intelligence and the future of surgical robotics*, Annals of Surgery, **270**, *2*, pp. 223–226, 2019.
3. PLITEA, N., HESSELBACH, J., VAIDA, C., RAATZ, A., PISLA, D., BUDDE, C., VLAD, L., BURISCH, A., SENNER, R., *Innovative development of surgical parallel robots*, Acta Electronica Mediamira Scientia, Cluj-Napoca, **4**, pp. 201–206, 2007.
4. GEORGE, E., I., BRAND, T., C., LaPORTA, A., MARESCAUX, J., SATAVA, R., M., *Origins of robotic surgery: from skepticism to standard of care*, JSLS: Journal of the Society of Laparoendoscopic Surgeons, **22**, *4*, e2018.00039, 2018.
5. CORNEJO, J., PERALES-VILLARROEL, P., SEBASTIAN, R., CORNEJO-AGUILAR, J., A., *Conceptual design of space biosurgeon for robotic surgery and aerospace medicine*, In 2020 IEEE ANDESCON, pp. 1–6, 2020.
6. ZHANG, W., LI, H., CUI, L., ZHANG, X., FANG, S., ZHANG, Q., *Research progress and development trend of the surgical robot and surgical instrument arm*, The International Journal of Medical Robotics and Computer Assisted Surgery, **17**, *5*, e2309, 2021.
7. MARCUS, H., J., RAMIREZ, P., T., KHAN, D., Z., LAYARD HORSFALL, H., HANRAHAN, J., G., WILLIAMS, S., C. *et al*., *The IDEAL framework for surgical robotics: development, comparative evaluation, and long-term monitoring*, Nature medicine, **30**, *1*, pp. 61–75, 2024.
8. FERRO, M., MIRANTE, A., FICUCIELLO, F., VENDITTELLI, M., *A CoppeliaSim dynamic simulator for the da Vinci research kit*, IEEE Robotics and Automation Letters, **8**, *1*, pp. 129–136, 2022.
9. WEI, B., ZHANG, D., *A review of dynamic balancing for robotic mechanisms*, Robotica, **39**, *1*, pp. 55–71, 2021.
10. GARBENS, A., MORGAN, T., CADEDDU, J., A., *Single port robotic surgery in urology*, Current Urology Reports, **22**, *4*, article 22, 2021.
11. HUTCHINS, A., R., MANSON, R., J., LEREBOURS, R., FARJAT, A., E., COX, M. L., MANN, B., P., ZANI, S., *Objective assessment of the early stages of the learning curve for the senhance surgical robotic system*, Journal of Surgical Education, **76**, *1*, pp. 201–214, 2019.
12. HUSCHER, C., MARCHEGIANI, F., COBELLIS, F., TEJEDOR, P., PASTOR, C., LAZZARIN, G., WHEELER, J., DI SAVERIO, S., *Robotic oncologic colorectal surgery with a new robotic platform (CMR Versius): hope or hype? A preliminary experience from a full-robotic case-series*, Tech. Coloproctol., **26**, pp. 745–753, 2022.
13. PISLA, D., BIRLESCU, I., CRIȘAN, N., PUSCA, A., ANDRAȘ, I., TUCAN, P., RADU, C., GHERMAN, B., VAIDA, C., *Singularity analysis and geometric optimization of a 6-dof parallel robot for SILS*, Machines, **10**, *9*, 764, 2022.
14. RUS, G., ANDRAS, I., VAIDA, C., CRISAN, N., GHERMAN, B., RADU, C., TUCAN, P., IAKAB, S., AL HAJJAR, N., PISLA, D., *Artificial intelligence-based hazard detection in robotic-assisted single-incision oncologic surgery*, Cancers, **15**, *13*, article 3387, 2023.
15. VAIDA, C., ANDRAS, I., BIRLESCU, I., CRISAN, N., PLITEA, N., PISLA, D., *Preliminary control design of a single-incision laparoscopic surgery robotic system*, Proc. of 25th Int. Conf. on System Theory, Control and Computing (ICSTCC), Iasi, Romania, pp. 384–389, 2021.
16. PISLA, D., PLITEA, N., VIDEAN, A., PRODAN, B., GHERMAN, B., LESE, D., *Kinematics and design of two variants of a reconfigurable parallel robot*, in: Proceedings of the ASME/IFToMM International Conference on Reconfigurable Mechanisms and Robots, London, UK, 24 July 2009.
17. SADEGHIAN, H., ZOKAEI, F., HADIAN JAZI, S., *Constrained Kinematic Control in Minimally Invasive Robotic Surgery Subject to Remote Center of Motion Constraint*, J. Intell. Robot. Syst., **95**, pp. 901–913, 2019.

18. TUCAN, P., VAIDA, C., ULINICI, I., BANICA, A., BURZ, A., POP, N., BIRLESCU, I., GHERMAN, B., PLITEA, N., ANTAL, T., et al., *Optimization of the ASPIRE Spherical Parallel Rehabilitation Robot Based on Its Clinical Evaluation*, International Journal of Environmental Research and Public Health, **18**, 3281, 2021, https://doi.org/10.3390/ijerph18063281.
19. VAIDA, C., BIRLESCU, I., PUSCA, A., GHERMAN, B., TUCAN, P., ANTAL, T., A., PISLA, D., *Geometric Modeling of a New Modular Spherical Robotic System for Single Incision Laparoscopic Surgery*, in: MÜLLER, Andreas, BRANDSTÖTTER, Michael (Eds), *Advances in service and industrial robotics*, Proc. Int. Conf. RAAD 2022; Mechanisms and Machine Science, **120**, pp. 367–374, 2022.
20. SHIN, H., J., SEO, S., W., LEE, Da Hyun, LEE, Mee-Ran, *Robotic single-port surgery using the da Vinci SP® surgical system for benign gynecologic disease: A preliminary report*, Journal of Minimally Invasive Gynecology, **27**, *1*, pp. 139–145, 2020, https://doi.org/10.1016/j.jmig.2019.08.018.
21. KUNZ, L., *A Review of the Role of Robotics in Surgery: To da Vinci and Beyond,* ResearchGate Preprint, November 2023, Available at: https://www.researchgate.net/publication/375447953, available online 20.08.25.
22. CMR SURGICAL, Versius Overview – Product Brochure, Cambridge, UK, Promedica-Praha, June 2023. Available at: https://www.promedica-praha.cz – available online 20.08.25.
23. FDA, Decision Summary DEN230078: Versius Surgical System, United States Food and Drug Administration, Center for Devices and Radiological Health, 2023.
24. ASENSUS SURGICAL, Senhance Surgical System – System Description and Features, 2023.,Available at: https://www.asensus.com/senhance, available online 20.08.25.
25. RUS, G., VAIDA, C., VANTA, O., MURESAN, A. *et al*., *The Control Architecture of a Spherical Robot for Minimally Invasive Surgery*, In: LOVASZ, E.C., CECCARELLI, M., CIUPE, V. (Eds), *Mechanism design for robotics* (MEDER), 2024; Mechanisms and Machine Science, **166**, Springer, Cham, 2024, https://doi.org/10.1007/978-3-031-67383-2_45.